Bulk Properties of α-PbO From First-principle Self-consistent Calculations

O. Rubel[†] and A. Potvin[†]

[*]*Thunder Bay Regional Research Institute, 290 Munro St, Thunder Bay, Ontario, Canada*
[†]*Lakehead University, 955 Oliver Road, Thunder Bay, Ontario, Canada*

Abstract. Structural, elastic and cohesive properties of α-PbO (litharge) obtained from all-electron *ab initio* calculations are reported. The emphasis is made on the role of the exchange correlation functional in prediction of those properties. Peculiarities of the mesoscopic structure of α-PbO are linked with its cohesive properties.

Keywords: Lead monoxide, litharge, lattice constants, bulk modulus, cohesive energy, density functional theory, exchange-correlation functional
PACS: 61.50.Ah, 61.50.Lt, 62.20.D-

INTRODUCTION

Polycrystalline lead monoxide (PbO) has recently emerged as a favorable photoconducting material for direct conversion x-ray detectors [1, 2, 3]. Lead oxide also has a long history as a photoconductor for television camera pick-up tubes (Plumbicon) [4]. The good sensitivity of PbO to x-rays is a result of the high x-ray to charge conversion efficiency and the high absorption coefficient of PbO for this radiation. The first prototype of a large-area detector has been demonstrated by Simon *et al.* [1], thereby indicating that there are no technological barriers for covering large-area thin film transistor plates with PbO layers. However, higher dark currents due to the high applied voltage and a non-perfect temporal behavior (image lag and ghosting) currently prohibit the success of PbO direct conversion dynamic detectors [5].

Lead monoxide is known to occur in two polymorphic forms: a red tetragonal α form (litharge) and a yellow orthorhombic β form (massicot) [6]. Litharge is stable at ambient conditions [7] and, therefore, is technologically preferable [1]. Litharge has a layered crystal structure shown in Fig. 1, which is a tetragonal distortion of a CsCl-type structure [8]. Within each layer the oxygen atoms are sandwiched between two lead sublayers. In the resulting structure each lead atom is bound to four oxygen atoms forming a square pyramid with a lead atom at the apex, and each oxygen atom is surrounded tetrahedrally by four lead atoms [8]. Since oxygen can accommodate only two valence electrons from lead, the remaining two valence electrons on the metal side form a lone pair. The lone pairs play the key role in the explanation of the distorted (noncentrosymmetric) metal coordination observed in post-transition metal oxides, such as α-PbO [9, 10, 11, 12, 13].

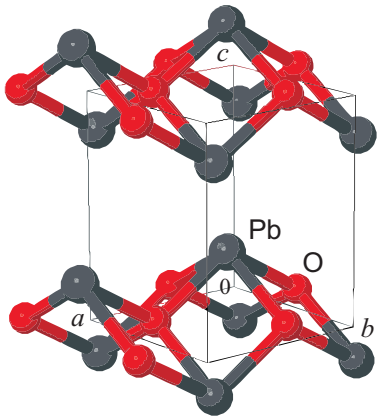

FIGURE 1. Atomic structure of α-PbO and its unit cell.

Advances in Mathematical and Computational Methods: Addressing Modern Challenges of Science, Technology, and Society
AIP Conf. Proc. 1368, 85-88 (2011); doi: 10.1063/1.3663466

First principle theoretical studies of lead monoxide are often limited to the electronic structure calculations performed at *experimental* lattice parameters [8]. The calculated lattice parameters of α-PbO reported in the literature [10, 11, 12] have an uncertainty of 10%, which exceeds the standard density-functional theory (DFT) accuracy for covalent solids by almost an order of magnitude. Furthermore, very few attempts have been made to calculate elastic [8] and cohesive properties [12] of α-PbO.

The purpose of our communication is to fill this gap by reporting structural, elastic and cohesive properties of α-PbO based on self-consistent all-electron DFT calculations.

CALCULATION DETAILS

Calculations of the electronic structure were performed in the framework of DFT using a full-potential linearized augmented plane-wave method implemented in WIEN2K package [14]. Two approximations for the exchange-correlation functional were used: the local density approximation (LDA) [15] and the generalized gradient approximation (GGA) [16].

The volume of a cell was partitioned onto nonoverlapping spheres with a radius of 2.0 and 1.6 Bohr centered at the nucleus of lead and oxygen atoms, respectively. The energy to separate core and valence states was set at -7.6 Ry that implies treatment of lead $5p$, $5d$, $6s$, $6p$ and oxygen $2s$, $2p$ electrons as valence ones. The product of the atomic sphere radius and plane-wave cutoff in k-space (the so-called RK_{max} parameter) was equal to 8.0. Such a high value is necessary in order to achieve convergence of the cohesive properties. Structural and elastic properties are well converged at the value of $RK_{max} = 7$.

The Brillouin zone of a primitive unit cell was sampled using $10 \times 10 \times 8$ Monkhorst-Pack mesh [17]. The less dense k-mesh $6 \times 6 \times 4$ also provides an adequate convergence of the calculated properties, however, the scattering of the total energy vs volume is less pronounced with the denser mesh.

The optimization of internal degrees of freedom (atomic positions) was performed for *every* realization. The optimization is based on minimization of Hellman-Feynman forces [18] and was continued until the forces acting on all atoms drop below 0.2 mRy/Bohr. This tight convergence criterion is essential for the total energy accuracy superior than 10^{-5} Ry.

TABLE 1. Bulk properties of α-PbO: the lattice constants a and c, the nearest-neighbor interatomic spacing $d_{\mathrm{Pb-O}}$, the bulk modulus B_0 and its pressure derivative dB_0/dP, and the cohesive energy E_{coh}.

	Present calculations		**Other calculations**		
Property	**GGA**	**LDA**	**GGA**	**LDA**	**Experimental values**
a_0 (Å)	4.055	3.947	4.06*	3.956,† 3.953**	3.96,‡ 3.975,§ 3.979¶
c_0 (Å)	5.677	4.887	5.39*	4.874,† 4.988**	5.02,‡ 5.023,§ 5.011¶
c/a	1.40	1.24	1.33*	1.23,† 1.26**	1.27,‡ 1.264,§ 1.26¶
$d_{\mathrm{Pb-O}}$ (Å)	2.35	2.30	2.35*	2.30**	2.32,‡ 2.31§
B_0 (GPa)	5.4 ± 0.7	23 ± 2	⋯	24.3†	23.1§, 24.8¶
dB_0/dP	16 ± 7	⋯	⋯	⋯	7.0§
E_{coh} (eV/atom)	4.4	5.2	5.5*	⋯	⋯

* Pseudopotentials, VASP code, GGA with semicore lead electrons [12]
† Pseudopotentials, VASP code, LDA without semicore lead electrons [10]
** Pseudopotentials, ABINIT code, LDA with semicore lead electrons [11]
‡ Leciejewicz [19]
§ Giefers and Porsch [20]
¶ Adams *et al.* [6]

RESULTS AND DISCUSSION

We begin with the calculation of structural properties of α-PbO by performing a two-dimensional optimization of the total energy with respect to the lattice parameters a and c. The optimal values obtained using LDA and GGA are listed in Table 1 along with the experimental results and results of other *ab initio* calculations. Apparently, GGA significantly underestimates an interaction between PbO layers resulting in the unrealistically large c/a ratio. On the other hand, LDA's a_0 and c_0 come much close to the experimental values than the corresponding GGA data. LDA slightly overestimates the bonding while maintaining c/a ratio almost at the experimental value.

Since the interactions within PbO layers have a covalent character, a_0 values calculated with LDA and GGA only slightly differ from their experimental counterpart. The same argument also applies to the Pb-O interatomic spacing with the layer. Similar trends can be observed in the results of other calculations performed using a pseudopotential technique (see Table 1).

Next, we proceed with calculation of elastic properties, namely the bulk modulus B_0. We determine the optimal c/a ratio as a function of the unit cell volume as illustrated in the insert to Fig. 2 for GGA. In the range of $\pm 6\%$ deviation from the equilibrium volume, the optimal c/a ratio increases linearly with increasing the volume. We emphasize once again that the full relaxation of atomic positions is essential for every structural realization. By choosing the optimal c/a ratio for every volume, the total energy variation vs volume is determined as shown in Fig. 2 (triangles). The bulk modulus is extracted by fitting these data to Murnaghan's equation of state.

Obtained results for the bulk modulus are listed in Table 1. The LDA bulk modulus is consistent with the experimental data as well as with the former theoretical calculations. The GGA largely underestimates the bulk modulus due to its failure to account for the interaction between PbO layers. This interaction is responsible for the relative large pressure derivative of the bulk modulus observed experimentally [20]. Our GGA calculations also suggest the anomalously high pressure derivative of the bulk modulus. Unfortunately, we were not able to resolve the derivative accurately enough in the case of LDA due to the data scattering.

Finally, we report calculation results for cohesive properties of α-PbO. The cohesive energy is defined as a difference between the total energy of α-PbO unit cell and that of the free atoms. The spin polarization was included while undertaking the total energy calculations for the free atoms. Our cohesive energy of α-PbO is about 5 eV/atom (Table 1), which is in the typical range of $4-9$ eV/atom for covalent solids [21]. The difference between LDA and GGA results for the cohesive energy is of the order of 1 eV/atom, which is also typical for DFT studies of covalent solids [21].

In order to determine a contribution of the interlayer bonding to the cohesive energy, we performed the total

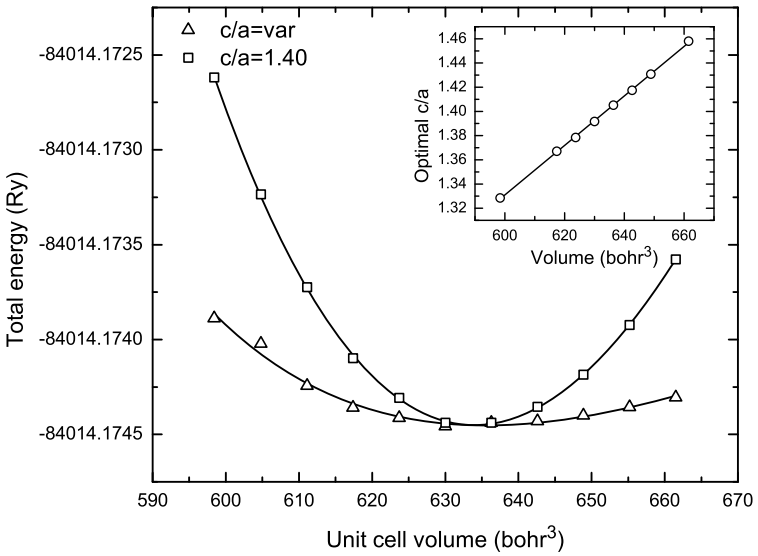

FIGURE 2. The total energy as a function of the unit cell volume of α-PbO calculated with GGA. Two scenarios are presented: (i) variable optimal c/a ratio as illustrated in the inset, and (ii) fixed c/a ratio. The second scenario, being physically unrealistic, results in a significant overestimation of elastic properties.

energy calculation of a structure with doubled separation between PbO layers. As a result, we can conclude that the contribution of the interlayer bonding to the cohesive energy is only about 2%. This result suggests that α-PbO has a very low (001) surface energy that causes litharge to appear in a form of fine-dispersed porous textures that consist of intersecting thin two-dimensional platelets [1, 2, 3].

CONCLUSIONS

Self-consistent all-electron *ab initio* calculations of structural, elastic and cohesive properties of α-PbO (litharge) are performed. The structural and elastic properties turn out to be very sensitive to the choice of the exchange correlation functional. We showed that GGA fails to account accurately for the interaction between adjacent PbO layers. In contrast to GGA, the LDA calculation results have much better agreement with the experimentally measured properties and, therefore, should be a preferable choice when undertaking *ab initio* calculations of α-PbO. Also we attribute the fine-dispersed porous structure of α-PbO with a low (001) surface energy resulting from the weak bonding between adjacent PbO layers.

ACKNOWLEDGMENTS

Financial support of the Natural Sciences and Engineering Research Council of Canada under a Discovery Grants Program “Microscopic theory of high-field transport in disordered semiconductors" is gratefully acknowledged.

REFERENCES

1. M. Simon, R. A. Ford, A. R. Franklin, S. P. Grabowski, B. Menser, G. Much, A. Nascetti, M. Overdick, M. J. Powell, and D. U. Wiechert, *Proc. SPIE* **5368**, 188 (2004).
2. M. Simon, R. A. Ford, A. R. Franklin, S. P. Grabowski, B. Menser, G. Much, A. Nascetti, M. Overdick, M. J. Powell, and D. U. Wiechert, “Analysis of lead oxide (PbO) layers for direct conversion X-ray detection,” in *IEEE Symposium Conference Record Nuclear Science 2004*, 2004, vol. 7.
3. M. Simon, R. A. Ford, A. R. Franklin, S. P. Grabowski, B. Menser, G. Much, A. Nascetti, M. Overdick, M. J. Powell, and D. U. Wiechert, *IEEE T. Nucl. Sci.* **52**, 2035 (2005).
4. L. Heijne, P. Schagen, and H. Bruining, *Nature* **173**, 220 (1954).
5. M. Z. Kabir, S. Kasap, and J. Rowlands, *Springer Handbook of Electronic and Photonic Materials*, Springer, 2006, chap. Photoconductors for x-ray image detectors, pp. 1121–1137.
6. D. M. Adams, A. G. Christy, J. Haines, and S. M. Clark, *Phys. Rev. B* **46**, 11358 (1992).
7. W. B. White, F. Dachille, and R. Roy, *J. Am. Ceram. Soc.* **44**, 170 (1961).
8. H. J. Terpstra, R. A. de Groot, and C. Haas, *Phys. Rev. B* **52**, 11690 (1995).
9. G. W. Watson, S. C. Parker, and G. Kresse, *Phys. Rev. B* **59**, 8481 (1999).
10. G. W. Watson, and S. C. Parker, *J. Phys. Chem. B* **103**, 1258 (1999).
11. J.-M. Raulot, G. Baldinozzi, R. Seshadri, and P. Cortona, *Solid State Sci.* **4**, 467 (2002).
12. A. Walsh, and G. W. Watson, *J. Solid State Chem.* **178**, 1422 (2005).
13. D. J. Payne, R. G. Egdell, A. Walsh, G. W. Watson, J. Guo, P.-A. Glans, T. Learmonth, and K. E. Smith, *Phys. Rev. Lett.* **96**, 157403 (2006).
14. P. Blaha, K. Schwarz, G. K. H. Madsen, D. Kvasnicka, and J. Luitz, *Wien2k: An Augmented Plane Wave + Local Orbitals Program for Calculating Crystal Properties*, Karlheinz Schwarz, Techn. Universität Wien, Austria, 2001.
15. J. P. Perdew, and Y. Wang, *Phys. Rev. B* **45**, 13244 (1992).
16. J. P. Perdew, K. Burke, and M. Ernzerhof, *Phys. Rev. Lett.* **77**, 3865 (1996).
17. H. J. Monkhorst, and J. D. Pack, *Phys. Rev. B* **13**, 5188 (1976).
18. R. Yu, D. Singh, and H. Krakauer, *Phys. Rev. B* **43**, 6411 (1991).
19. J. Leciejewicz, *Acta Cryst.* **14**, 1304 (1961).
20. H. Giefers, and F. Porsch, *Physica B: Condensed Matter* **400**, 53 (2007).
21. P. P. Rushton, *Towards a non-local density functional description of exchange and correlation*, Ph.D. thesis, University of Durham (2002).